Cationic *O*-ethylphosphatidylcholines and their lipoplexes: phase behavior aspects, structural organization and morphology

Rumiana Koynova[*,1], Robert C. MacDonald

Department of Biochemistry, Molecular and Cell Biology, Northwestern University, 2205 Tech Drive, Evanston, IL 60208, USA

Abstract

Ethylphosphatidylcholines, positively charged membrane lipid derivatives in which the anionic charge of the phosphate oxygen has been eliminated by ethylation, are promising nonviral, metabolizable transfection agents. We studied in detail the phase behavior, structural organization and morphology of the ethylphosphatidylcholines and their lipoplexes. Unlike the other phospholipids, dehydration does not change the melting transition temperature of *O*-ethyl-dipalmitoylphosphatidylcholine (EDPPC). Neither does an isoelectric amount of DNA, when added to the EDPPC aqueous dispersion. This is ascribed to the inability of EDPPC to form hydrogen bonds because of its headgroup modification. Similarly to its parent lipid DPPC, EDPPC displays a subtransition at 15 °C in its differential scanning calorimetry (DSC) heating scans after prolonged low-temperature incubation. The cooling behavior of the *O*-ethylphosphatidylcholines is sensitive to the thermal prehistory and the ionic strength. Different aggregate morphologies in the solid and the liquid-crystalline phases—respectively lamellar sheets and vesicles, as documented by light microscopy—are considered responsible for the cooling pattern. The interconversion between these morphologies is slow or even kinetically hindered, however, increasing the ionic strength to physiological values facilitates the conversion. The interdigitated chain arrangement of EDPPC gel phase tolerates incorporation of DNA between the bilayers. The minimum observed separation between the DNA strands is ~ 30–32 Å, at DNA/lipid molar ratio ≥ 1. Formation of lipoplexes with DNA ordered in a 1-D lattice sandwiched between interdigitated lipid bilayers is reported for the first time.

1. Introduction

Because of their potential application in gene therapy and drug delivery applications [1,2], positively charged lipids are now being intensively synthesized and studied. However, comprehensive knowledge on the organization of cationic lipid aggregates, the process of cationic lipid–DNA assembly and the correlation between the structure and activity of these complexes is still deficient and the synthesis of new compounds for transfection is mostly empirical. Among the numerous cationic "lipoids" synthesized and tested recently, phosphatidylcholine triesters (Fig. 1) [3–5] are the only membrane lipid derivatives shown to be metabolized by cells. They are thus considered promising nonviral transfection agents. These compounds are chemically stable, hydrate well and form liposomes, which readily fuse with anionic lipid vesicles [6]. Numerous parameters of the preparation protocols are shown to modulate the structure and morphology of their complexes with DNA [7], which in turn influence their transfection activity, but all the liquid crystalline members of this group exhibit high transfection efficiency, provided proper attention is given to the mechanical aspects of lipoplex formation. The saturated ethyl-phosphatidylcholines have been shown to exhibit gel–liquid crystalline phase transitions at temperatures close to those of the parent phosphatidylcholines [3,8]. Below the transition, they arrange into a gel phase with interdigitated hydrocarbon chains [8,9]. Their liquid-crystalline phase is characterized by a significantly thinner water layer between the bilayers as compared to the phosphatidylcholines [9]. Here we report some additional details of the phase behavior of the saturated ethylphosphatidylcholines related to the different morphology of their aggregates in the gel and liquid crystalline phases, as well as the slow interconversion

---

* Corresponding author. Tel.: +1-847-491-2871; fax: +1-847-467-1380.

E-mail address: r-tenchova@northwestern.edu (R. Koynova).

[1] On leave of absence from the Institute of Biophysics, Bulgarian Academy of Sciences, 1113 Sofia, Bulgaria.
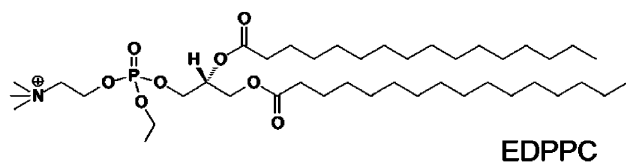
Fig. 1. Molecular structure of 1,2-dipalmitoyl-*sn*-glycero-3-ethylphosphocholine (EDPPC).

between them. Surprisingly, we found that the melting transition temperature of ethylphosphatidylcholines is neither changed by dehydration nor by addition of an isoelectric amount of DNA to their aqueous dispersions. We explored the structure of the *O*-ethyl-dipalmitoylphosphatidylcholine (EDPPC) lipoplexes in the gel and liquid crystalline phases and found that the interdigitated gel phase tolerates the inclusion of DNA between the bilayers.

2. Materials and methods

2.1. Lipids

Triflate derivatives of dipalmitoyl ethyl-phosphatidylcholine (EDPPC), dimyristoyl ethyl-phosphatidylcholine (EDMPC) and dioleoyl ethyl-phosphatidylcholine (EDOPC) were synthesized as previously described [3–5]. In some experiments, the chloride salt of EDPPC from Avanti Polar Lipids, Inc. (Birmingham, AL) was used. The triflate and the chloride salts of EDPPC were found to have the same calorimetric behavior and to form the same lamellar structures upon hydration. The phospholipids were found to migrate as a single spot when checked by thin-layer chromatography. They were stored at −20 °C in chloroform. Aliquots were transferred to vials where the bulk of the solvent was removed with a stream of argon. The vial was then placed under high vacuum for at least 1 h/mg lipid to remove residual chloroform. Next, the appropriate aqueous solution was added. The dispersions were hydrated overnight at 4 °C and cycled five to six times between ∼10 °C above the chain-melting transition and 0 °C (ice bath). The samples were vortexed at these temperatures for 1–2 min at each cycle. Lipid concentrations of stock solutions were determined using a phosphate assay [10].

The lipid concentrations of the dispersions were 1–3 mg/ml for calorimetry, and 5–20 wt.% for X-ray diffraction (XRD). For XRD measurements, samples were filled into glass capillaries (*d* = 1.0 or 1.5 mm) (Charles Super Co., Natick, MA) and flame-sealed with a butane microtorch.

2.2. DNA

Herring sperm DNA (Invitrogen, Carlsbad, CA), 10 mg/ml solution in water, was used. DNA/lipid dispersions for calorimetry were prepared by adding DNA solution dropwise to the preformed lipid dispersions. Samples were

equilibrated for 1–3 days before measurements. For X-ray samples, 5 wt.% lipid dispersions were sonicated to near-clarity at temperature 5–10 °C above the chain melting transition, DNA was added and the dispersions were equilibrated overnight. The samples were concentrated either by centrifugation or by lyophilization at −80 °C and rehydration. After sealing into capillaries, samples were temperature cycled several times between 60 °C and room temperature, and equilibrated for 5–7 days before measurements.

2.3. Differential scanning calorimetry (DSC)

High-sensitivity microcalorimetric measurements were performed using a VP-DSC Microcalorimeter (MicroCal Inc., Northampton, MA) [11]. Heating and cooling scans were performed at scan rates of 0.2–0.5 °C/min (4-s filtering). Thermograms were analyzed using MicroCal Origin software.

For dry samples, a DSC 550 (Instrument Specialists Incorporated, Spring Grove, IL) heat-flow calorimeter was used. Heating scans were performed at 1–2 °C/min.

2.4. Small-angle X-ray diffraction (SAXD)

Measurements were performed at Argonne National Laboratory, Advanced Photon Source, BioCAT (beamline 18-ID) and DND-CAT (beamline 5-IDD), using 12–15 keV X-rays. 2D diffraction patterns were recorded using high-sensitivity CCD detectors. Sample-to-detector distance was 1.8–2 m. Silver behenate (DuPont, Wilmington, DE) was used as a calibrant (d_{001} = 58.376 Å [12]). For temperature control, either a THMS600 thermal stage (Linkam Sci Instruments, Surrey, England) or a NESLAB programmable water bath (Thermo NESLAB, Portsmouth, NH) was used. Linear heating and cooling scans were performed at rates of 0.8–3 °C/min. Exposure times were typically 0.5–5 s.

SAXD measurements were also performed using Ni-filtered CuK_{α} radiation (λ = 1.5418 Å) from a rotating anode generator ELLIOTT-GX6 (Elliott Automation Radar Systems Ltd., Marconi Avionics, Herts, England). Sample-to-detector distance was typically ∼380 mm. Diffraction patterns were recorded on a Bruker HI-STAR area detector (Bruker AXS, Inc., Madison, WI) controlled by computer using GADDS software. The sample temperature was regulated with laboratory-built sample holder using a thermoelectric Peltier element. Typical exposure time was ∼1 h. The 2D diffraction patterns did not show angular dependence of the scattered intensity for the studied phases. Diffraction intensity vs. reciprocal space *s* plots were obtained by radial integration of the 2D patterns using the interactive data-evaluating program FIT2D [13,14]. Some samples with longer exposure time were checked by thin layer chromatography after the experiments. Products of lipid degradation were not detected in these samples, and radiation damage of the lipids was not evident from their X-ray patterns.

2.5. Light microscopy

Micrographs of lipid samples were taken using a light microscope (Nikon Optiphot) using differential interference optics. Images were recorded with a video camera (MTI 65) connected to a personal computer by means of a Studio DC10 Plus (Pinnacle Systems, Inc., Mountain View, CA) video capturing system. Preformed samples were placed on microscope slides and were covered with a glass coverslip, hermetic sealed with Vaseline (not contacting the sample).

3. Results and discussion

3.1. Details of the phase behavior of the cationic ethyl-PCs

3.1.1. Dry EDPPC

Hydrated EDPPC has been reported to undergo a melting transition at $T_m = 42$ °C, with an enthalpy change of 9.6 kcal/mol [3,8,9]. According to our calorimetric data, dry EDPPC samples (lyophilized from aqueous dispersion) exhibited a melting transition at virtually the same temperature, with a slightly lower enthalpy change of ~ 8 kcal/mol (Fig. 2A). This transition was between two lamellar phases, with lamellar repeat periods d of 39.4 Å (20 °C) and 41.8 Å (50 °C), respectively, as revealed by SAXD (Fig. 2B and C).

The short lamellar repeat distance suggests that EDPPC assumes an interdigitated gel phase in the dry state. It should

be recognized that in the dry state, each EDPPC molecule has a large co-anion (triflate) which may have to be taken into account in consideration of the structure and thermodynamic properties of the lipid.

Preservation of the chain-melting transition temperature of EDPPC upon dehydration is noteworthy, for the precursor lipid, DPPC, exhibits a nearly 30 °C increase of the transition temperature upon dehydration to DPPC-dihydrate [15,16]. In fact, an increase in the chain-melting transition temperature upon dehydration below the "excess water" limit is observed in virtually all phospholipids that have been studied. Such stabilization is believed to be brought about by additional inter- and intrabilayer hydrogen bonding in the dehydrated state [17]. The lack of a similar increase of T_m in EDPPC is possibly a result of the absence of hydrogen bonding, due to the phosphate group modification. Because of this behavior, ethyl-PCs constitute a useful reference for estimating the effect of hydrogen bonding on different aspects of the phospholipid behavior.

The values of the lamellar repeat distances in the gel and liquid crystalline phases of the dry EDPPC are 2.6–3 Å smaller than the respective bilayer thicknesses in the hydrated state, as estimated from the electron density profiles [9]. This is possibly an indication that dehydration causes some rearrangement of the lipid organization, in addition to the removal of the water layers between the lipid bilayers. Several phenomena could produce such bilayer thinning: (i) Reorientation of the headgroups. Such rearrangement is usually related to inter- or intramolecular
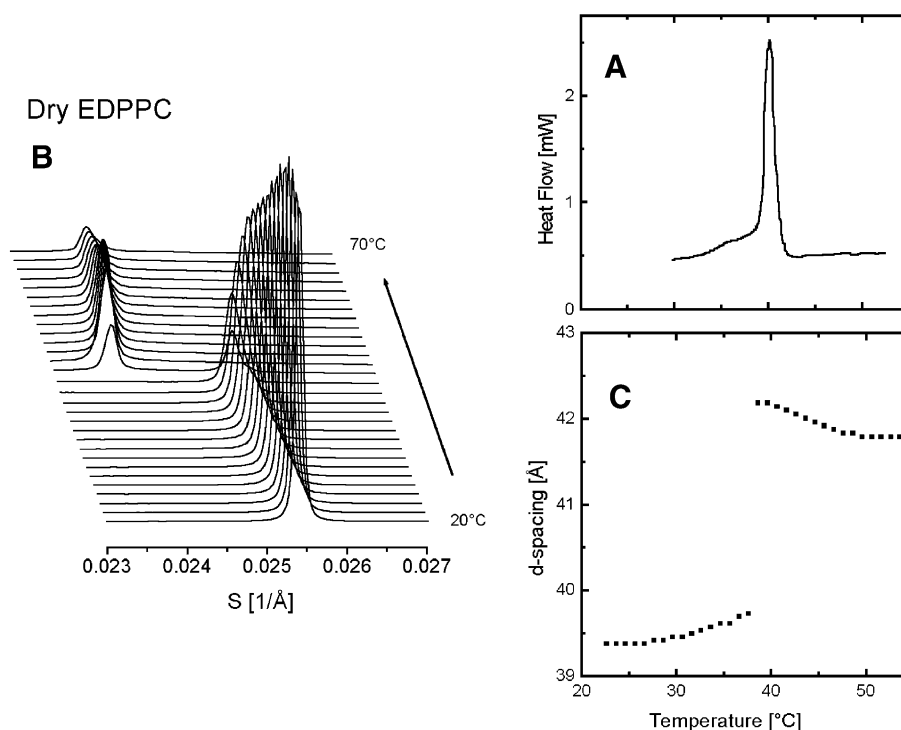

Fig. 2. (A) DSC heating thermogram of lyophilized EDPPC recorded at 1 °C/min; (B) SAXD patterns recorded upon heating at 1 °C/min of a dry (lyophilized from aqueous dispersion) EDPPC sample (exposure time 2 s); (C) lamellar repeat spacing as a function of temperature.

hydrogen bonding and thus is less probable in this case; (ii) Additional interdigitation to the point where the terminal methyl groups of hydrocarbon chains of the one lipid layer level out with the headgroups of the opposing layer of the lipid bilayer. Such layout is certainly unfavorable in aqueous dispersion, but may become favorable in the dry state. Such a rearrangement was prompted by the fact that the bilayer contraction of 2.6 Å in the dry gel state matches the thickness of $2CH_2$ groups, i.e., one additional step of interdigitation along the hydrocarbon zigzag. (iii) Tilting of the hydrocarbon chains at $\sim 30°$ might bring about a ~ 2.6-Å bilayer thinning—a possibility that might be checked by wide-angle X-ray diffraction. The possibility of increased chain interdigitation seems to us most probable because it would also account for the bilayer contraction in the liquid crystalline phase, in which the interdigitation seems to be partially preserved, as judged by its short lamellar spacing. In this regard, it is worth noting that dihexadecylphosphatidylcholine (DHPC), the ether analogue of DPPC, which also forms spontaneously interdigitated gel phase in aqueous dispersion, undergoes a transformation to a non-interdigitated gel phase when dehydrated [18,19]. This difference in the phase behavior presumably reflects the different origin of the chain interdigitation in the DHPC and EDPPC aqueous dispersions; in DHPC it is probably produced by the mismatch between the hydrated head group cross-sectional area and that of the hydrocarbon chains, whereas in EDPPC it is more of electrostatic origin.

3.2. Low-temperature sub-transition in hydrated ethyl-PCs

When dispersed in water, cationic ethyl-PCs with saturated acyl chains of 14–18 C-atoms are known to form an interdigitated lamellar gel phase, which undergoes a thermal phase transition to a lamellar liquid crystalline phase at temperatures close to those of the melting transitions of the parent PC compounds [8,9]. Except for the melting gel–liquid crystalline transition, the phosphatidylcholines themselves also exhibit several other transitions between various gel and subgel polymorphic phases (see, e.g., Ref. [20] for a review). One of them, the transition to a more ordered low-temperature gel phase with orthorhombic chain arrangement [21,22], referred to as the 'Y-transition', which seems to be characteristic for a wide collection of saturated phospho- and glycolipids [23], was also noticed in the ethylated PCs with saturated 16- and 18-C atom chains [8,9]. In addition, we report that another transition typical for the saturated PCs, namely the subtransition, is also observed in the ethyl-PC derivatives.

When stored at low temperature for a prolonged time (several days), EDPPC exhibits a transition at ~ 15 °C, with a maximum enthalpy of ~ 2 kcal/mol that is reached after 10–12 days of equilibration (Fig. 3). It is not observed on the subsequent cooling–heating scans and thus resembles the DPPC sub-transition (subgel–gel transition) [24].
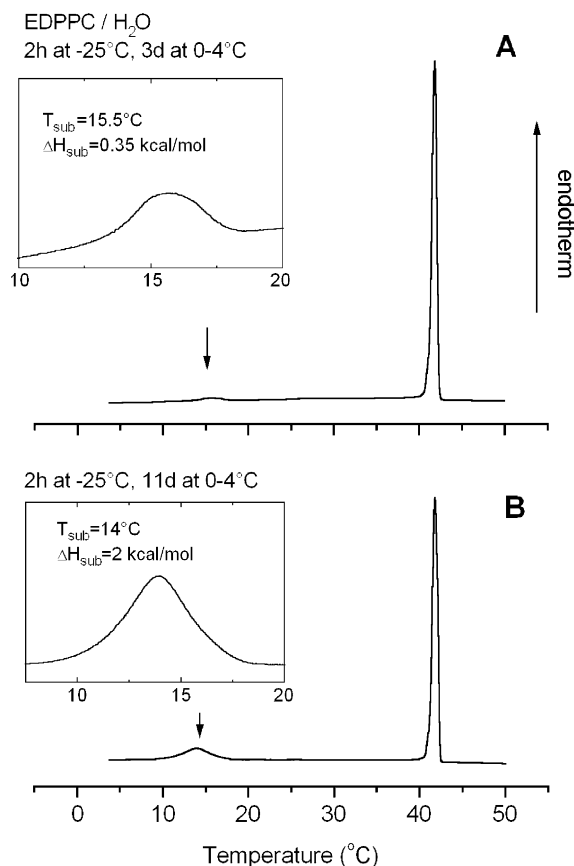

Fig. 3. DSC thermograms of EDPPC aqueous dispersions recorded at 0.5 °C/min; the samples were frozen at -25 °C for 2 h, and then stored at $0-4$ °C for (A) 3 days and (B) 11 days. Insets give expanded view of the subtransition region indicated by the arrow.

Indeed, it has been shown that chain interdigitation does not prevent the formation of a subgel phase [21][2].

3.3. Cooling behavior

It was noticed previously that the cooling thermograms of aqueous dispersions of ethyl-PCs exhibit double exotherms, which were both assigned to the transformation from the liquid crystalline phase to the interdigitated gel phase [8,9]. This feature is considered typical for dispersions forming interdigitated gel phases, and has been ascribed to the existence of two different gel-phase morphologies [28]. In fact, splitting of the cooling transition has also been observed in phosphatidylethanolamines, which do not form interdigitated gel phases (e.g., Refs. [29,30]), so we believe it is a more general phenomenon.

---

[2] Our recent DSC data imply that chain interdigitation does not obstruct another transition typical for the long-chain saturated PCs either: the sub-main transition [24], which is believed to reflect a decoupling of the events of a loss of conformational acyl-chain order (chain melting) and loss of the translational lateral order, thus representing a 'solid ordered-liquid ordered' transition on heating [25–27], and which typically occurs at $1-2$ °C below the main transition, seems to take place in EDSPC as well.

Here we provide additional information regarding the cooling behavior of ethyl-PC aqueous dispersions. In Fig. 4A, the double-exotherm cooling DSC pattern of an EDPPC/H$_2$O sample is shown. Our synchrotron X-ray data confirmed that only the continuous coexistence of the initial lamellar liquid crystalline phase and the final interdigitated gel phase existed within the temperature interval between the two cooling exotherms (Fig. 5). Further, sequentially recorded DSC cooling thermograms demonstrated a redistribution of enthalpy of the cooling exotherms, with the high-temperature exotherm strongly dominating after equilibration of the sample at low-temperature prior to the experiment, and the low-temperature exotherm growing in enthalpy with each cycle through the main transition. Noteworthy is that such cycling did not result in final elimination of the high-temperature exotherm—after the initial five to six cycles, the enthalpy ratio did not undergo further change. Similar behavior was shown for EDMPC/H$_2$O sample upon the initial two cooling scans (Fig. 4B). After the second cooling, the sample was heated to 30 °C, taken out of the calorimeter and vortexed for 1 min at that temperature, and then the third and fourth cooling thermograms were recorded sequentially. As may be seen in the figure, only the low-temperature exotherm was then observed. It took at least 1 day of low-temperature equilibration before the high-temperature cooling exotherm appeared again in the thermograms.

In Fig. 4C and D, the cooling pattern of EDPPC and EDMPC in 150 mM PBS (pH 7.2) is compared to that in water. For EDPPC, even on the first cooling the low-temperature exotherm dominated strongly in PBS (Fig. 4C), and it was the only one present on the subsequent cooling thermograms. For EDMPC, the low-temperature exotherm also dominated the first cooling but there was still considerable presence of the high-temperature exotherm. The latter was eliminated after high-temperature vortexing (Fig. 4D).

The morphological background of the recorded thermal behavior was revealed from light micrographs taken at room temperature (Fig. 6). The EDPPC dispersion in water
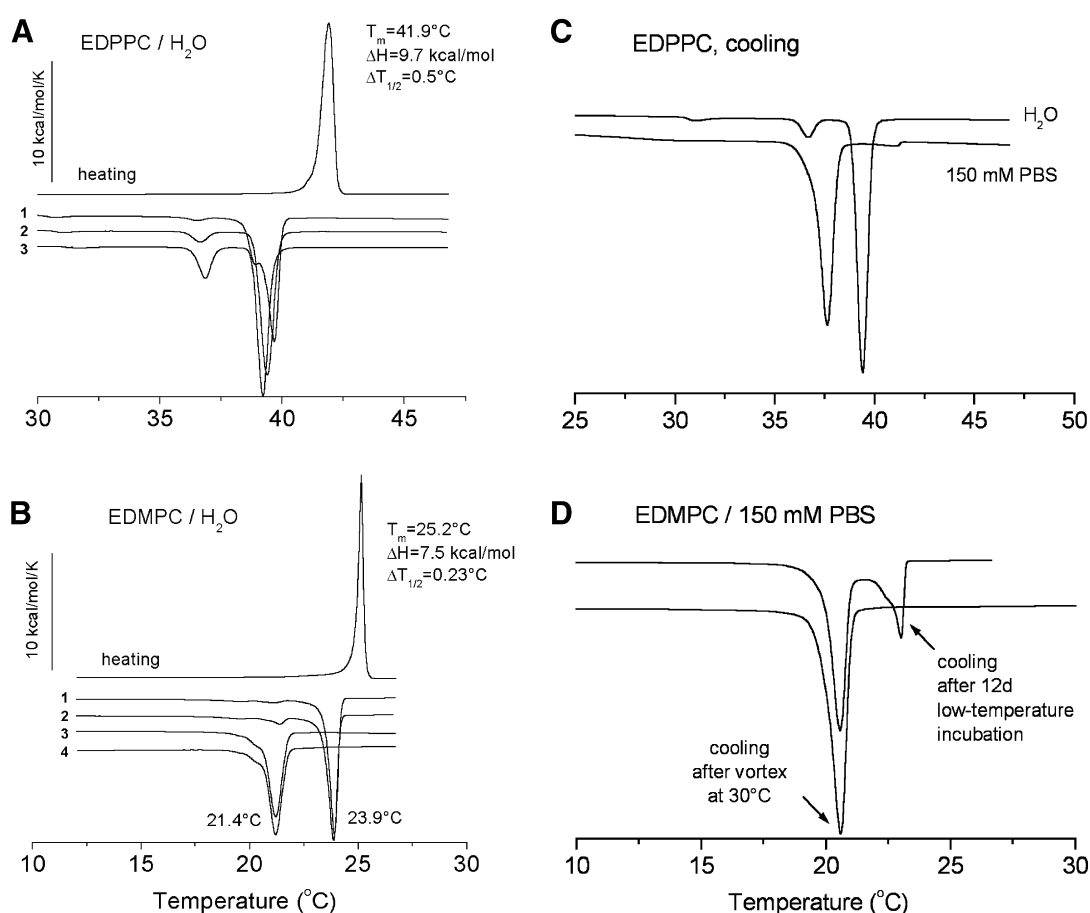

Fig. 4. DSC thermograms of EDPPC and EDMPC dispersions recorded following different protocols: (A) Initial heating (after 5d at 0–4 °C) and three sequential cooling thermograms of EDPPC/H$_2$O dispersion. (B) Initial heating (after 4 days at 0–4 °C) and sequential cooling thermograms of EDMPC aqueous dispersion. After the third heating, the sample has been taken out of the calorimeter and vortexed at 35 °C for 1 min, then third and fourth cooling thermograms have been recorded. (C) Cooling thermograms of EDPPC dispersions in H$_2$O and 150 mM PBS. (D) Cooling thermograms of EDMPC dispersions in 150 mM PBS recorded immediately after heating of a sample, stored for 12 days at 0–4 °C, and after vortexing the sample at 30 °C for 1 min. Scan rate 0.5 °C/min.
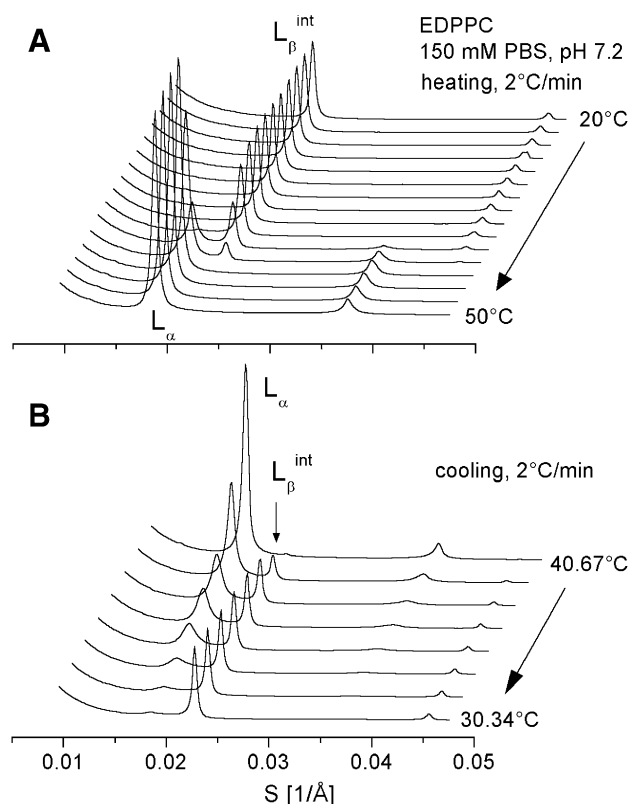
Fig. 5. SAXD patterns of EDPPC sample in 150 mM PBS (pH 7.2) recorded on (A) heating and (B) cooling at 2 °C/min.

displayed large aggregates after long low-temperature storage (Fig. 6A-1). It should be emphasized that these aggregates consist in large part of extended bilayers, not of individual vesicles. These were preserved mostly unchanged after single heating through the melting transition and immediate cooling back to room temperature (Fig. 6A-2), but were completely transformed into small, spherical liposomes after vortexing the dispersion above the transition (Fig. 6A-3). In 150 mM PBS, the transformation of the large aggregates into smaller liposomes largely occurred during the first cooling, even without high-temperature vortexing (Fig. 6B).

These data indicate a different morphology of the lipid in the gel and liquid crystalline phases, namely extended lamellar stacks and small vesicles, respectively. Moreover, while the phase transition is fast in terms of chain melting↔solidification (half-times of the order of milliseconds have been reported), the transition between the two macroscopic morphologies is either rather slow and takes place within days (liposome → stack conversion), or is kinetically hindered and can be triggered by mechanical agitation (stack → liposome conversion). Interestingly, the heating behavior of the two kinds of aggregates is identical, whereas their cooling transition temperatures differ by some 2–3 °C, i.e., the vesicle phase transition is characterized by much larger temperature hysteresis. It is noteworthy that the presence of electrolyte considerably accelerates the interconversion between the two types of lipid aggregates. Chart
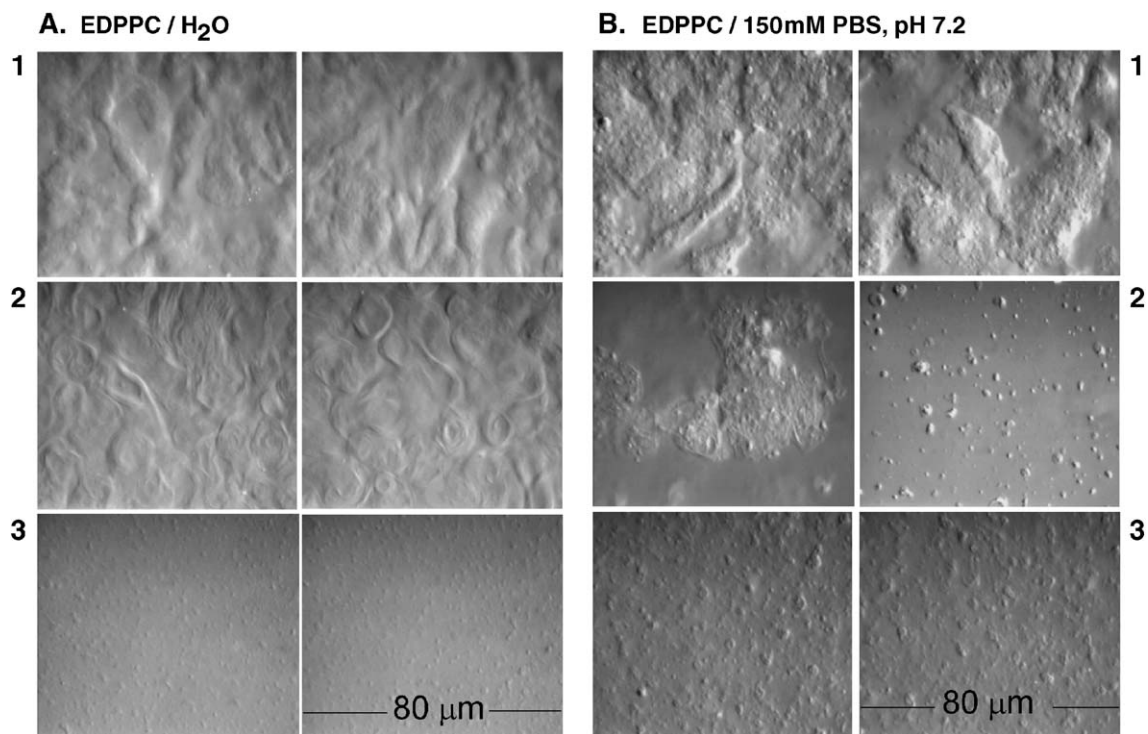

Fig. 6. Micrographs of EDPPC samples in (A) H$_2$O and (B) 150 mM PBS, taken at room temperature (∼ 22 °C) after (1) 15-day incubation at 0–4 °C; (2) heating to 50 °C without mechanical agitation; (3) vortexing for 1 min at 50 °C.

of the morphological changes and pathways is shown in Fig. 7.

3.4. Ethyl-PC/DNA lipoplexes

3.4.1. EDOPC/DNA

In the presence of DNA, the structural organization of the EDOPC aggregates was still lamellar, according to our SAXD results. Increase of the lamellar repeat distance by ~ 16 Å was observed (Fig. 8C), in agreement with previous data [3,31]. In addition to the lipid lamellar reflections, another low-intensity diffuse peak was present on the diffraction patterns (Fig. 8D). Such a peak has been interpreted as reflecting the in-plane packing of the DNA strands intercalated between the lipid lamellae [32–34]. Its spacing was 50 Å in the DNA/EDOPC 1:4 sample, decreasing to 32 Å in the 1:1 and 2:1 samples (Fig. 8C). Similar limiting values of the DNA interaxial separation have been previously reported for DOTAP/DOPC and DMTAP/DMPC lipoplexes [32–36].

3.4.2. EDPPC/DNA

Addition of an isoelectric amount of DNA to the aqueous EDPPC dispersions did not change noticeably the thermodynamic characteristics of their gel–liquid crystalline phase transition—the transition temperature was virtually the same, 41.6 ± 0.23 °C, and the transition enthalpy was only decreased by about 15–20%, to ~ 8 ± 1 kcal/mol. Precise determination of the transition enthalpy was obstructed by the high inhomogeneity of the dispersion produced upon the addition of DNA. As seen from the structural data presented below, EDPPC did incorporate DNA and formed lipoplexes. Similarly to the case of the dry EDPPC bilayers discussed above, the reason for preservation of the transition temperature in the presence of DNA is probably the inability of EDPPC to form hydrogen bonds. Thus, the incorporation of DNA in the interbilayer space does not significantly perturb the thermodynamics of the EDPPC bilayer phase transition.

In order to gain insight on the effect of the lipid gel–liquid crystalline phase transition on the structure of the ethyl-PC lipoplexes, we performed SAXD experiments with the saturated EDPPC. Its lamellar repeat period increased as a function of the DNA content both in the gel and liquid crystalline phases as shown in Fig. 8A. Even small amounts of DNA (DNA/EDPPC 1:4 molar ratio) sharply increased (by ~ 12 Å) the lamellar repeat distance, suggesting the formation of lipoplexes with DNA sandwiched between lipid bilayers (Fig. 8B). The lamellar repeat distance grew further at 1:2 molar ratios, then slightly decreased in the 1:1 samples. This was probably a result of a better ordering in the equimolar complexes. Further increasing the DNA content resulted in additional growth of the repeat distance, with a splitting of the lamellar reflections at a twofold excess of DNA. The increase of the lamellar spacing of the liquid crystalline phase of EDPPC by 12–15 Å by the presence of DNA was similar to that for EDOPC. Moreover, we observed similar
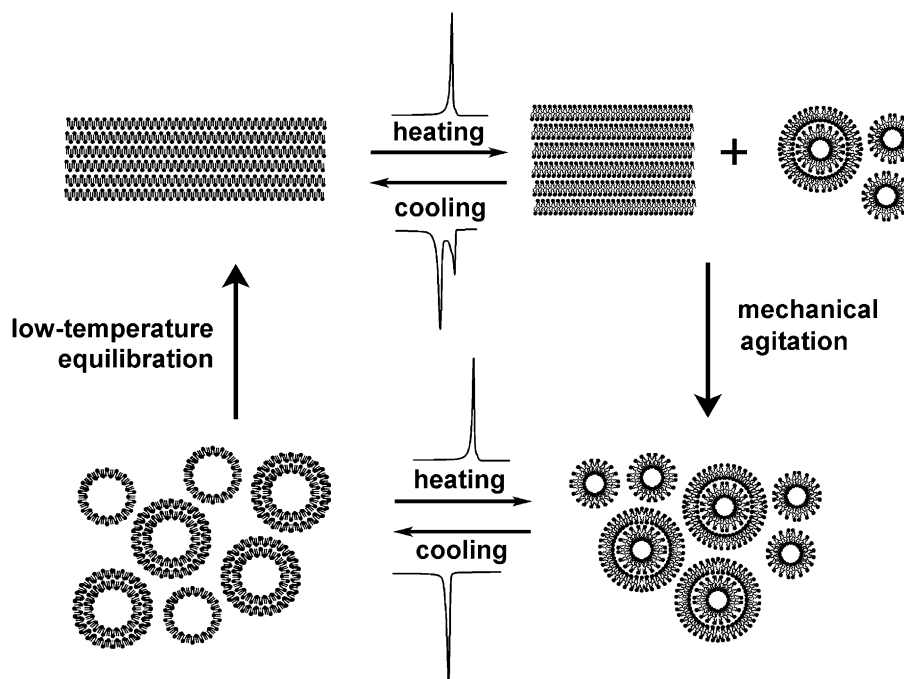

Fig. 7. Diagram of the morphological changes in EDPPC dispersions. The equilibrium low-temperature arrangement appears to be lamellar sheets, with chain interdigitation. Upon heating, liposomes and lamellar sheets (both non-interdigitated) coexist, whose mixture fully converts into liposomes (apparently the equilibrium liquid crystalline phase arrangement) only after mechanical treatment. Cooling back to the gel phase produces gel-phase liposomes which convert back into lamellar sheets only after prolonged low-temperature exposure.
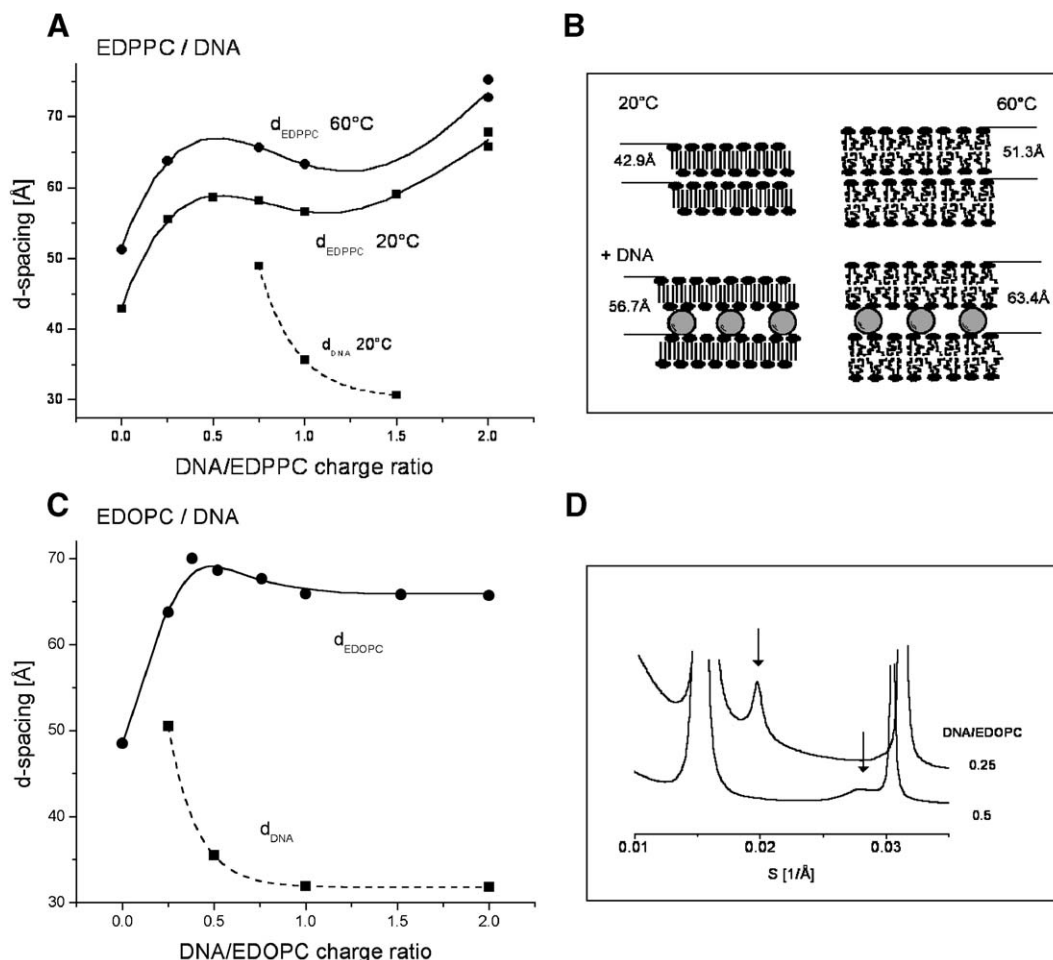
Fig. 8. (A) Lamellar lipid spacing, d_{EDPPC}, and DNA repeat distance, d_{DNA}, of EDPPC/DNA samples as a function of the DNA/lipid molar (charge) ratio at 20 and 60 °C, as determined from SAXD experiments. (B) Proposed molecular arrangement. (C) Lipid lamellar repeat spacing, d_{EDOPC}, and DNA repeat distance, d_{DNA}, in EDOPC/DNA lipoplexes as a function of the molar ratio. (D) SAXD patterns at DNA/EDOPC samples at 1:2 and 1:4 molar ratio (arrows point at the peaks originating from the DNA–DNA in-plane correlation).

increase of the d-spacing also in the gel phase. This is indicative that incorporation of the DNA strands between the EDPPC lamellae is characteristic also for the lipid gel phase. Such a view is supported also by the presence of the diffuse peak supposedly originating from the lattice of the DNA strands intercalated between the lipid lamellae (Fig. 8A). Formation of a condensed lipid/DNA lamellar gel phase has been previously documented for mixed DMTAP/DMPC bilayers [35]. The expansion of the lamellar gel phase by ∼ 15 Å in the lipid/DNA samples suggests that the chain interdigitation typical for the EDPPC gel phase has not been disrupted by the inclusion of the DNA strands between the lipid lamellae. Indeed, were the DNA incorporation accompanied by transformation of the condensed gel phase into a non-interdigitated one, an additional increase of the d-spacing by at least 10 Å would be expected (see, e.g., Ref. [9], for the structural parameters of the EDPPC phases compared to the DPPC). It thus appears that the interdigitated lamellar lipid arrangement in the gel phase of EDPPC tolerates the sandwiched lipid–DNA structure

(Fig. 8B) proposed for non-interdigitated DOTAP/DOPC bilayers [32,33,37].

The coexistence of two sets of lamellar reflexes in the sample with 2:1 DNA/lipid ratio is suggestive for the appearance of another population of lipid/DNA aggregates of different organization at excess DNA compositions. Interestingly, formation of two different populations of aggregates at different charge ratios was recently proposed for DOTAP lipoplexes also [38].

4. Conclusions

1. Thermodynamic parameters of the gel–liquid crystalline phase transition of the hydrated EDPPC are virtually unchanged upon dehydration or in the presence of DNA. Thus, dry EDPPC exhibits a melting transition at the same temperature as when fully hydrated or when involved in lipoplexes. This is taken to be a consequence of the inability of ethyl-PCs to form hydrogen bonds.

2. The interdigitated chain arrangement typical for the hydrated EDPPC gel bilayers is preserved and even probably enhanced in the dry state.

3. The cooling behavior of the hydrated EDMPC and EDPPC is sensitive to the sample history. It reflects the existence of two types of lipid aggregates—lamellar sheets and vesicles, the former being the equilibrium state for the gel phase, and the latter—for the liquid crystalline phase. The interconversion between these different morphologies is slow and probably kinetically hindered; it thus does not correlate well with the much faster chain melting transition. Formation of lamellar sheets is promoted by low-temperature standing, while their conversion to vesicles is promoted by high-temperature mechanical agitation. High ionic strength facilitates the sheet-to-vesicle conversion.

4. Similarly to its precursor DPPC, EDPPC exhibits a subtransition after a prolonged low-temperature exposure.

5. In the EDOPC/DNA complexes, DNA is ordered in a 1-D lattice sandwiched between the lipid bilayers. The interaxial spacing of DNA decreases from 50 Å at a DNA/EDOPC 1:4 charge ratio to 32 Å in the 1:1 and 2:1 samples.

6. When added to EDPPC, DNA incorporates into the interbilayer space both in the gel and in the liquid crystalline phase, and increases the lamellar repeat distance by $12-15$ Å. In the gel phase, the lipid chain interdigitation seems to be preserved, and the limiting DNA interaxial separation is ~ 30 Å. Such complexes of DNA sandwiched between interdigitated gel lipid bilayers are reported for the first time. In compositions containing excess DNA, another population of lipid/DNA aggregates of different organization possibly forms.

References

[1] P.L. Felgner, G.M. Ringold, Cationic liposome-mediated transfection, Nature 337 (1989) 387–388.

[2] P.L. Felgner, Nonviral strategies for gene therapy, Sci. Am. 276 (1997) 102–106.

[3] R.C. MacDonald, G.W. Ashley, M.M. Shida, V.A. Rakhmanova, Y.S. Tarahovsky, D.P. Pantazatos, M.T. Kennedy, E.V. Pozharski, K.A. Baker, R.D. Jones, H.S. Rosenzweig, K.L. Choi, R. Qiu, T.J. McIntosh, Physical and biological properties of cationic triesters of phosphatidylcholine, Biophys. J. 77 (1999) 2612–2629.

[4] R.C. MacDonald, V.A. Rakhmanova, K.L. Choi, H.S. Rosenzweig, M.K. Lahiri, O-ethylphosphatidylcholine: a metabolizable cationic phospholipid which is a serum-compatible DNA transfection agent, J. Pharm. Sci. 88 (1999) 896–904.

[5] H. Rosenzweig, V.A. Rakhmanova, T.J. McIntosh, R.C. MacDonald, O-Alkyl dioleoylphosphatidylcholinium compounds: the effect of varying alkyl chain length on their physical properties and in vitro DNA transfection activity, Bioconjug. Chem. 11 (2000) 306–313.

[6] D.P. Pantazatos, R.C. MacDonald, Directly observed membrane fusion between oppositely charged phospholipid bilayers, J. Membr. Biol. 170 (1999) 27–38.

[7] M.T. Kennedy, E.V. Pozharski, V.A. Rakhmanova, R.C. MacDonald, Factors governing the assembly of cationic phospholipid–DNA complexes, Biophys. J. 78 (2000) 1620–1633.

[8] R.N.A.H. Lewis, I. Winter, M. Kriechbaum, K. Lohner, R.N. McElhaney, Studies of the structure and organization of cationic lipid bilayer membranes: calorimetric, spectroscopic, and X-ray diffraction studies of linear saturated P-O-ethyl phosphatidylcholines, Biophys. J. 80 (2001) 1329–1342.

[9] I. Winter, G. Pabst, M. Rappolt, K. Lohner, Refined structure of 1,2-diacyl-P-O-ethylphosphatidylcholine bilayer membranes, Chem. Phys. Lipids 112 (2001) 137–150.

[10] G.R. Bartlett, Phosphorus assay in column chromatography, J. Biol. Chem. 234 (1959) 466–468.

[11] V.V. Plotnikov, J.M. Brandts, L.-N. Lin, J.F. Brandts, A new ultrasensitive scanning calorimeter, Anal. Biochem. 250 (1997) 237–244.

[12] T.N. Blanton, T.C. Huang, H. Toraya, C.R. Hubbard, S.B. Robie, D. Louër, H.E. Göbel, G. Will, R. Gilles, T. Raftery, JCPDS-international centre for diffraction data round robin study of silver behenate. A possible low-angle X-ray diffraction calibration standard, Powder Diffr. 10 (1995) 91–95.

[13] A.P. Hammersley, ESRF Internal Report, ESRF98HA01T (1998), FIT2D V9.129 Reference Manual V3.1.

[14] A.P. Hammersley, S.O. Svensson, M. Hanfland, A.N. Fitch, D. Häusermann, Two-dimensional detector software: from real detector to idealised image or two-theta scan, High Press. Res. 14 (1996) 235–248.

[15] M. Kodama, M. Kuwabara, S. Seki, Successive phase transition phenomena and phase diagram of the phosphatidylcholine–water system as revealed by differential scanning calorimetry, Biochim. Biophys. Acta 689 (1982) 567–570.

[16] C. Grabielle-Madelmont, R. Perron, Calorimetric studies on phospholipid–water systems I, DL-Dipalmitoylphosphatidylcholine (DPPC)–water system, J. Colloid Interface Sci. 95 (1983) 471–482.

[17] J.M. Boggs, Lipid intermolecular hydrogen bonding: influence on structural organization and membrane function, Biochim. Biophys. Acta 906 (1987) 353–404.

[18] P. Laggner, K. Lohner, G. Degovics, K. Müller, A. Schuster, Structure and thermodynamics of the dihexadecylphosphatidylcholine–water system, Chem. Phys. Lipids 44 (1987) 31–60.

[19] J.T. Kim, J. Mattai, G.G. Shipley, Gel phase polymorphism in ether-linked dihexadecylphosphatidylcholine bilayers, Biochemistry 26 (1987) 6592–6598.

[20] R. Koynova, M. Caffrey, Phases and phase transitions of the phosphatidylcholines, Biochim. Biophys. Acta MR, Rev. Biomembr. 1376 (1998) 91–145.

[21] J.L. Slater, C.-H. Huang, Scanning calorimetry reveals a new phase transition in L-α-dipalmitoylphosphatidylcholine, Biophys. J. 52 (1987) 667–670.

[22] R. Koynova, B.G. Tenchov, S. Todinova, P.J. Quinn, Rapid reversible formation of a metastable subgel phase in saturated diacylphosphatidylcholines, Biophys. J. 68 (1995) 2370–2375.

[23] B. Tenchov, R. Koynova, G. Rapp, New ordered metastable phases between the gel and subgel phases in hydrated phospholipids, Biophys. J. 80 (2001) 1873–1890.

[24] S.C. Chen, J.M. Sturtevant, B.J. Gaffney, Scanning calorimetric evidence for a third phase transition in phosphatidylcholine bilayers, Proc. Natl. Acad. Sci. U. S. A. 77 (1980) 5060–5063.

[25] K. Jørgensen, Calorimetric detection of a sub-main transition in long-chain phosphatidylcholine lipid bilayers, Biochim. Biophys. Acta 1240 (1995) 111–114.

[26] M. Nielsen, L. Miao, J.H. Ipsen, K. Jørgensen, M.J. Zuckermann, O.G. Mouritsen, Model of a sub-main transition in phospholipid bilayers, Biochim. Biophys. Acta 1283 (1996) 170–176.

[27] K. Pressl, K. Jørgensen, P. Laggner, Characterization of the sub-main transition in distearoylphosphatidylcholine studied by simultaneous small- and wide-angle X-ray diffraction, Biochim. Biophys. Acta 1325 (1997) 1–7.

[28] J. Mason, R.E. Cunningham, T.J. O'Leary, Lamellar phase polymorphism in interdigitated bilayer assemblies, Biochim. Biophys. Acta 1236 (1995) 65–72.

[29] R.M. Epand, R.F. Epand, Kinetic effects in the differential scanning calorimetry cooling scans of phosphatidylethanolamines, Chem. Phys. Lipids 49 (1988) 101–104.

[30] H. Yao, I. Hatta, R. Koynova, B. Tenchov, Time-resolved X-ray diffraction and calorimetric studies at low scan rates. II. On the fine structure of the phase transitions in hydrated DPPE, Biophys. J. 61 (1992) 683–693.

[31] V.A. Rakhmanova, T.J. McIntosh, R.C. MacDonald, Effect of dioleoylphosphatidylethanolamine on the activity and structure of O-alkyl phosphatidylcholine–DNA transfection complexes, Cell. Mol. Biol. Lett. 5 (2000) 51–65.

[32] D.D. Lasic, H. Strey, M.C.A. Stuart, R. Podgornik, P.M. Frederik, The structure of DNA–liposome complexes, J. Am. Chem. Soc. 119 (1997) 832–833.

[33] J.O. Rädler, I. Koltover, T. Salditt, C.R. Safinya, Structure of DNA–cationic liposome complexes: DNA intercalation in multi-lamellar membranes in distinct interhelical packing regimes, Science 275 (1997) 810–814.

[34] T. Salditt, I. Koltover, J.O. Rädler, C.R. Safinya, Two-dimensional smectic ordering of linear DNA chains in self-assembled DNA–cationic liposome mixtures, Phys. Rev. Lett. 79 (1997) 2582–2585.

[35] R. Zantl, F. Artzner, G. Rapp, J.O. Rädler, Thermotropic structural changes of saturated-cationic-lipid–DNA complexes, Europhys. Lett. 45 (1998) 90–96.

[36] I. Koltover, T. Salditt, J.O. Rädler, C.R. Safinya, An inverted hexagonal phase of DNA–cationic liposome complexes related to DNA release and delivery, Science 281 (1998) 78–81.

[37] T. Boukhnikachvili, O. AguerreChariol, M. Airiau, S. Lesieur, M. Ollivon, J. Vacus, Structure of in-serum transfecting DNA–cationic lipid complexes, FEBS Lett. 409 (1997) 188–194.

[38] C.M. Wiethoff, M.L. Gill, G.S. Koe, J.G. Koe, C.R. Middaugh, The structural organization of cationic lipid–DNA complexes, J. Biol. Chem. 277 (2002) 44980–44987.